4.1 Introduction

Iron is an essential element required for many physiological processes in human body such as oxygen transport, electron transfer, gene regulation, and regulation of cell growth and differentiation. It also acts as a co-factor in many enzymatic reactions (Zhang and Du 2016). The deficiency of iron results in several diseases such as anemia, methemoglobinemia, low blood pressure and decreased immunity etc (Gao *et al*. 2015, Park *et al*. 2016). However, an excessive intake of iron leads to several pathological diseases such as Alzheimer, Huntington and Parkinson by accelerating the production of reactive oxygen species via the Fenton reaction (Altamura and Muckenthaler 2009, Uttara *et al*. 2009, Thatai *et al*. 2014). Therefore, the development of rapid, economic efficient, accurate and sensitive methods is very necessary from environmental as well as human health point of view.

Since last few years, several analytical techniques have been reported for the detection of iron such as atomic absorption spectrometry, inductively coupled plasma mass spectrometry and inductively coupled plasma emission spectrometry. But these techniques need sophisticated instrumentation, technical expertise and tedious sample preparation. Hence; these are not economic efficient and user friendly. Recently, the colorimetric detection technique is being extensively utilized to detect the metal ions in aqueous solution because of cost-efficient and less time-consuming procedures (Lee *et al*. 2014). Recently, the noble metal nanoparticles (NMNPs) and its composite have received great interest of the researchers because of potential applications in various fields such as; catalysis, biosensing, electronics water treatment, antimicrobial formulations, wound dressings, medicine, and surgical instruments (Yola *et al*. 2014a, Yola *et al*. 2014b, Yola *et al*. 2016a, Atar *et al*. 2015a, Atar *et al*. 2015b, Eren *et al*. 2015, Gupta *et al*. 2013, Yola *et al*. 2016b). At present,

NMNPs are being utilized extensively in colorimetric detection of metal ion due to high surface plasmon resonance (SPR), stable dispersion, biocompatibility and tunable physical and chemical properties (Dong *et al*. 2014). Among these NMNPs, AgNPs has strongest surface plasma resonance. Therefore, most of the sensing applications and SPR-related fundamental investigations have focused on AgNPs. Several articles have been reported on the colorimetric detection of pollutants using AgNPs. Kumar *et al*. has reported the colorimetric detection of melamine from water using unmodified AgNPs (Kumar *et al*. 2016a). Colorimetric detection of sulfide using chitosan-capped silver nanoparticles was reported by Shanmugaraj and Ilanchelian (Shanmugaraj and Ilanchelian 2016). Shrivas *et al*. have reported the sensitive colorimetric detection of chromium (Shrivas *et al*. 2016). He and Zhang reported the ultrasensitive colorimetric detection of manganese (II) ions (He and Zhang 2016). AgNPs conjugated with aptamers was also used to detect arsenic (Divsar *et al*. 2015).

AgNPs have been synthesized by several routes such as physical, chemical and biological (Rao and Paria 2013). Sputter deposition, laser ablation or cluster beam deposition are the physical routes of nanoparticles synthesis, but these processes need sophisticated instrumentation and technical expertise for the operation (Chen *et al*. 2003). The chemical reduction, electrochemical techniques and photochemical reductions are most widely used chemical approaches for AgNPs synthesis but the use of organic solvents, and toxic reducing agents have limited the applicability and ideality of this approach (Durán *et al*. 2011, Gade *et al*. 2014). Green synthesis approach has emerged out as a new eco-friendly and economically viable route to avoid the problems related to chemical and physical route (Das *et al*. 2011, Saxena *et al*. 2012). It has been performed either by microbial or herbal route (Iravani 2011,

Kowshik *et al*. 2002, Mandal *et al*. 2006, Mukherjee *et al*. 2001). The microbial route is not suitable for scale up at industrial level due to the requirement of external supply of nutrients, maintenance of highly aseptic conditions and technical expertise (Kumar *et al*. 2014). Recently, herbal route for the nanoparticles synthesis using plant extracts is potentially advantageous over microbial route because of its simple, economical and eco-friendly nature. It requires less time and eliminates the need of culture, aseptic conditions and maintenance (Bar *et al*. 2009, Zargar *et al*. 2014, Jayaseelan *et al*. 2013, Shankar *et al*. 2004). It has been reported that plant extracts contain various phytochemicals such as terpenoids, flavonoids, tannin, phenol derivatives, plant enzymes, protein and reducing sugars. These phytochemicals of herbal extracts act as both reducing as well as capping agent required for the synthesis and stabilization of nanoparticles (Kumar *et al*. 2016b, Jacob and Shalaev 2011, Thakkar *et al*. 2010).

Among the various green synthetic routes, the herbal route driven by the sunlight proved to be more economical and eco-friendly for the size controlled biosynthesis of the AgNPs using an aqueous extract of leaves (Amaladhas *et al*. 2013, Quaresma *et al*. 2009, Zhang *et al*. 2010). There are several articles which have been published for the biosynthesis of AgNPs using sunlight induced route. Zarchi *et al*. have reported the rapid biosynthesis of AgNPs using ethanol extract of *Andrachnea chordifolia* via sunlight-induced route (Zarchi *et al*. 2011). Dong *et al*. produced a stepwise synthesis of AuNPs under solar radiation (Dong *et al*. 2004). Biosynthesis of AgNPs was reported by Sahu *et al*. using an aqueous extract of *Cynodon dactylon* under bright sunlight radiation (Sahu *et al*. 2013).

C. bonplandianum, a plant of Euphorbiaceae family, is a native weed to the Southern Bolivia, Paraguay, Southwestern Brazil and Northern Argentina. It is also found in India as

an exotic weed and commonly found along the roads, canal and other water-stressed area. In spite of having medicinal value it has a great composition of reducing as well as capping agent required for the potent biosynthesis of AgNPs (Kumar *et al*. 2016b, Vadlapudi 2010). *C. bonplandianum*, commonly known as Three-Leaved Caper. It has been reported that extracts from different parts of this plant possess various medicinal value against Jaundice, Acute Constipation, Abdominal Dropsy and Internal Abscesses and also restrain antimicrobial and antitumor activity (Reddy 1988, Dutta and Ray 2014).

The prime objective of the present study is the optimum synthesis of stable AgNPs by optimizing several process parameters to investigate the selective colorimetric detection of Fe^{3+}. The antibacterial and antioxidant property of AgNPs was also investigated. It was also tried to avoid the use of any toxic chemical, technical expertise, sophisticated instrumentation, heating and stirring as well in the synthesis of AgNPs to make it completely eco-friendly, economic and nonhazardous.

4.2 Materials and method

4.2.1 Preparation of leaf extract

The collected leaves of the *C. bonplandianum* (**Fig. 4.1A**) were washed thoroughly with UPW, dried under shade and chopped into small pieces. Then 25 g of fine pieces of leaves were boiled for 5 min at 100 °C in 100 mL of UPW. After cooling, the extract was collected by decanting and filtered through Whatman filter paper No. 1. The prepared aqueous extract of *C. bonplandianum* (AEC) was stored as a stock solution at 4 °C and used within 3 days (**Fig. 4.1B**). The confirmation and quantification of total polyphenolic compounds were carried out using 'Ferric chloride test' and 'Folin Ciocalteu's method' respectively which are discussed in chapter 2 under section 2.3.2.

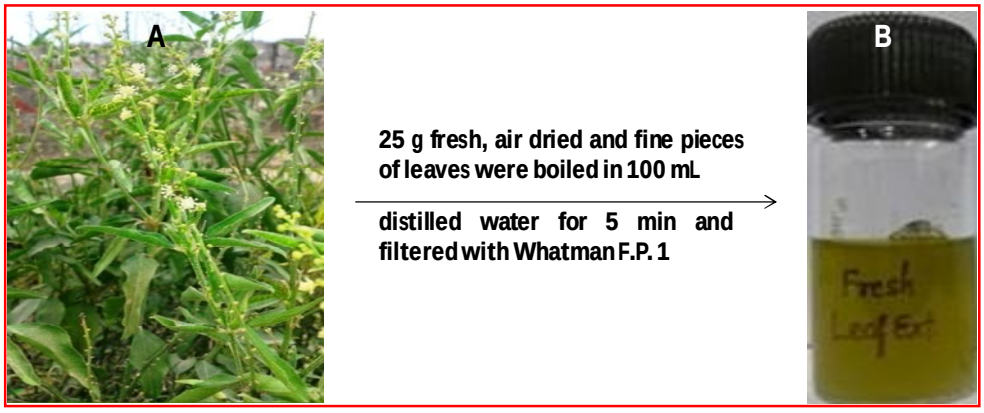

Figure 4.1 (A) *Croton bonplandianum* plant, (B) Aqueous extract of *Croton bonplandianum* (AEC)

4.2.2 Synthesis of AgNPs

Initially, the experiments were conducted with two sets of reaction mixtures each having 100 mL of 1 mM $AgNO_3$ solution and AEC inoculum dose of 2.5% (v/v). The $AgNO_3$ concentration and inoculum dose were selected arbitrarily. The first sets of reaction mixture were exposed to bright sunlight between 12 am and 2 pm for avoiding the fluctuations in solar intensity while other sets were kept in a black colored sealed vessel at dark conditions. The temperature of the ambient environment in bright sunlight and solar intensity were 38 °C and 530 lux respectively while the temperature of the dark condition and solar intensities were 30 °C and 0 lux respectively. The pH of the reaction mixture was neutral. The first sets exposed to bright sunlight showed an instant color change from greenish yellow to reddish brown within few seconds whereas the reaction mixture kept at dark condition exhibited only a slight change in color up to 12 hrs which indicated the photocatalytic action of sunlight on the synthesis of AgNPs. Therefore, further all the AgNPs synthesis experiments were conducted in bright sunlight in order to optimize the process

variables using one factor at a time approach. The process variables used for the optimization purpose were screened in the following range; duration of sunlight exposure from 0-30 min, AEC inoculum dose from 2.5% to15.0% (v/v) and $AgNO_3$ concentration from 1 mM to 6 mM. After the completion of the reaction at these optimized conditions the synthesized AgNPs were purified. For purification purpose the reaction mixture was centrifuged at 15000 rpm for 15 min and subsequently redispersed in UPW to eliminate the uncoordinated biological molecules. This process was repeated four times and after drying the final mass of AgNPs was collected.

4.2.3 Experimental methodology

The biosynthesis of AgNPs was monitored using UV–Visible spectroscopy (Evolution 201, Thermo Scientific) in the range of 300 to 700 nm. For the spectroscopic measurement, 200 µL aliquots of colloidal AgNPs was taken in 3 cm cuvette and diluted by adding 3 mL UPW. Fourier transform infrared spectroscopy (FTIR) was carried out in the range of 4000–400 cm^{-1} using FTIR spectrophotometer (Perkin Elmer Spectrum 100) to screen the involved functional groups in biosynthesis and stabilization of AgNPs. The crystalline nature of AgNPs was determined by using an X-ray Diffractometer (Rigaku HR-XRD, SMART Lab, Johnson Optics having Dtex ultra 250 detector) at a wide range of Bragg angles 2θ at a scanning rate of 5° min^{-1}. The morphology and size of nanoparticles were initially determined by Field Emission Scanning Electron Microscopy (FE-SEM Hitachi H-7100) at accelerating voltage of 10 kV, beam current 1 nA and typical measuring time of 7 second. For FE-SEM determination, one drop of colloidal AgNPs was dried over a small piece of thin aluminium sheet for two hrs under a table lamp. The detailed and precise morphology and size of the synthesized AgNPs were further explored by High-Resolution

Transmission Electron Microscopy (HR-TEM) analysis. The HR-TEM was carried out on TECNAI 20 G2-electron microscope operated at accelerating voltage 200 kV by drop coating of colloidal AgNPs on the carbon-coated copper grid. The surface texture was analyzed by Atomic Force Microscopy (AFM) using NT-MDT working in the contact mode. The AFM images have been processed using NOVA software. The purity of the AgNPs was determined by Energy Dispersive X-Ray Spectroscopy (EDX) which was equipped with FE-SEM as mentioned above. The X-Ray Photoelectron Spectroscopy (XPS) was conducted for the speciation of AgNPs. The XPS spectra were recorded with the AMICUS, Kratos Analytical, A Shimadzu with Mg Ka (1253.6 eV) radiation as X-ray source. The synthesized AgNPs was investigated for the colorimetric detection of iron (III), antibacterial and antioxidant activity which are given in detail in chapter 2 under section 2.5

4.3 Results and discussion

4.3.1 Primary confirmation of synthesis of AgNPs

The primary sign of biosynthesis of AgNPs was the change in color of the reaction mixture from greenish yellow to reddish brown. The reaction mixture exposed to bright sunlight exhibited an instant color change whereas the reaction mixture kept at dark condition did not attain the same color change even after 24 hrs (**Fig. inset 4.2A & 4.2B**). The bright sunlight exposed samples turned reddish brown within few seconds and dark brown within 40 seconds of AEC inoculation into $AgNO_3$ solution. This change in color was the primary indication of AgNPs synthesis which was confirmed by the presence of SPR band at 442 nm within 10 second whereas the reaction mixture kept at dark did not exhibit any SPR band even after 24 hrs **(Fig. 4.2A & B)**.

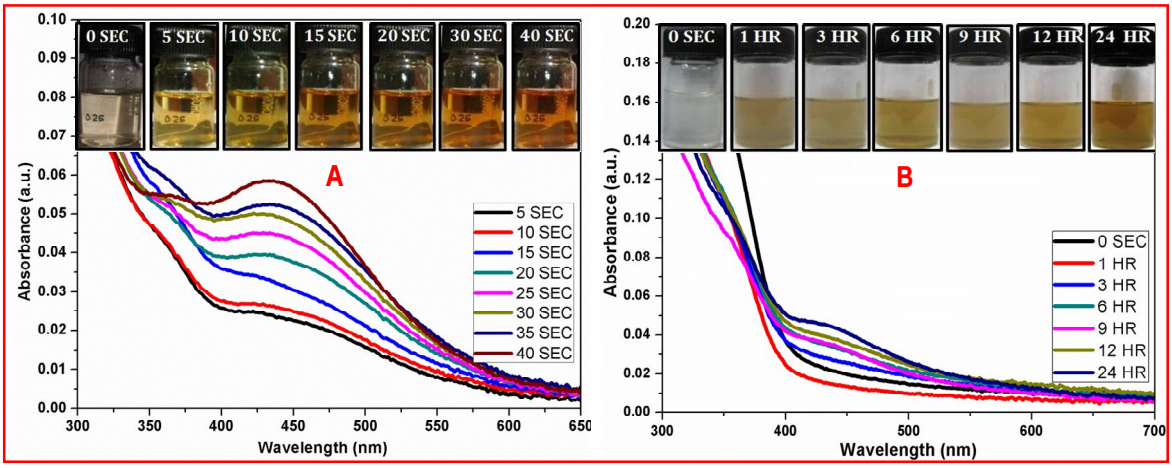

Figure 4.2 (A) UV–visible absorption spectra of AgNPs recorded in bright sunlight at 5, 10, 15, 20, 30, and 40 second (from 5 to 40 second), conditions; $AgNO_3$ conc. 1 mM, AEC inoculum dose 2.5% (v/v), (Inset Figure 4.2A) instant change from watery to brown and gradual increase in color of reaction mixture in bright sunlight up to 40 second, (B) UV–visible absorption spectra of AgNPs recorded in dark condition at different time interval (from 0 second to 24 hrs), conditions; $AgNO_3$ conc. 1 mM, AEC inoculum dose 2.5% (v/v), (Inset Figure 4.2B) change in color of reaction mixture recorded at different time intervals in dark conditions up to 24 hrs

This time lag clearly showed that the reaction was photocatalytic in nature. The appearance of color in the reaction mixture was due to surface plasmon resonance which arose through collective oscillations of free conduction electrons enforced by an interacting electromagnetic field (Kumar *et al*. 2016c). The samples were withdrawn from the reaction mixture at a regular time interval of five min and screened between 300 to 700 nm using UV-visible spectroscopy. The screening of samples taken from the reaction mixture after five min of sunlight exposure showed a sharp SPR band at 433 nm which attributed to the characteristic surface plasmon resonance of AgNPs having λ_{max} values in the range of 400-500 nm (Saravanan and Nanda 2010) **(Fig. 4.3A)**. According to various scientific reports, the SPR absorbance depends on the nature, surrounding media, shape and size of the

nanoparticles (Jagtap and Bapat 2013). According to a well-known theory, the absorption spectra of spherical nanoparticles result into a single SPR band whereas variation in the shape of the particles results into two or more SPR bands (Kumar *et al*. 2016b). In the current study, the reaction mixtures showed a single SPR band indicating the spherical shape of biosynthesized AgNPs which was further confirmed by FE-SEM and HR-TEM analysis. Such a green route of AgNPs synthesis is completely economic efficient as well as eco-friendly because of avoiding instruments, hazardous reducing agents, heating and stirring as well.

4.3.2 Optimization of process parameters

4.3.2.1 Sunlight duration

The experiments were conducted to optimize the exposure time by keeping the reaction mixture in bright sunlight under monitoring and results are shown in **Figure 4.2A & 4.3A-F**. The reaction mixtures exposed to bright sunlight showed an instant color change within few seconds (**Inset Fig. 4.2A**). This change in color of the reaction mixture was consistent with the UV-visible absorption spectra of the samples and the single SPR band at 428 nm after 30 min of sunlight exposure was characteristic of spherical AgNPs (Hou *et al*. 2013). As the time proceeded the color of the reaction mixtures became darker and the intensity of the SPR bands increased which signified the greater reduction of Ag^{+} to Ag^{0} (Birla *et al*. 2013). To optimize the effect of sunlight on the synthesis of AgNPs, firstly, the reaction mixtures were screened at each 5 second and then at each 5 min of interval to avoid a large number of SPR band.

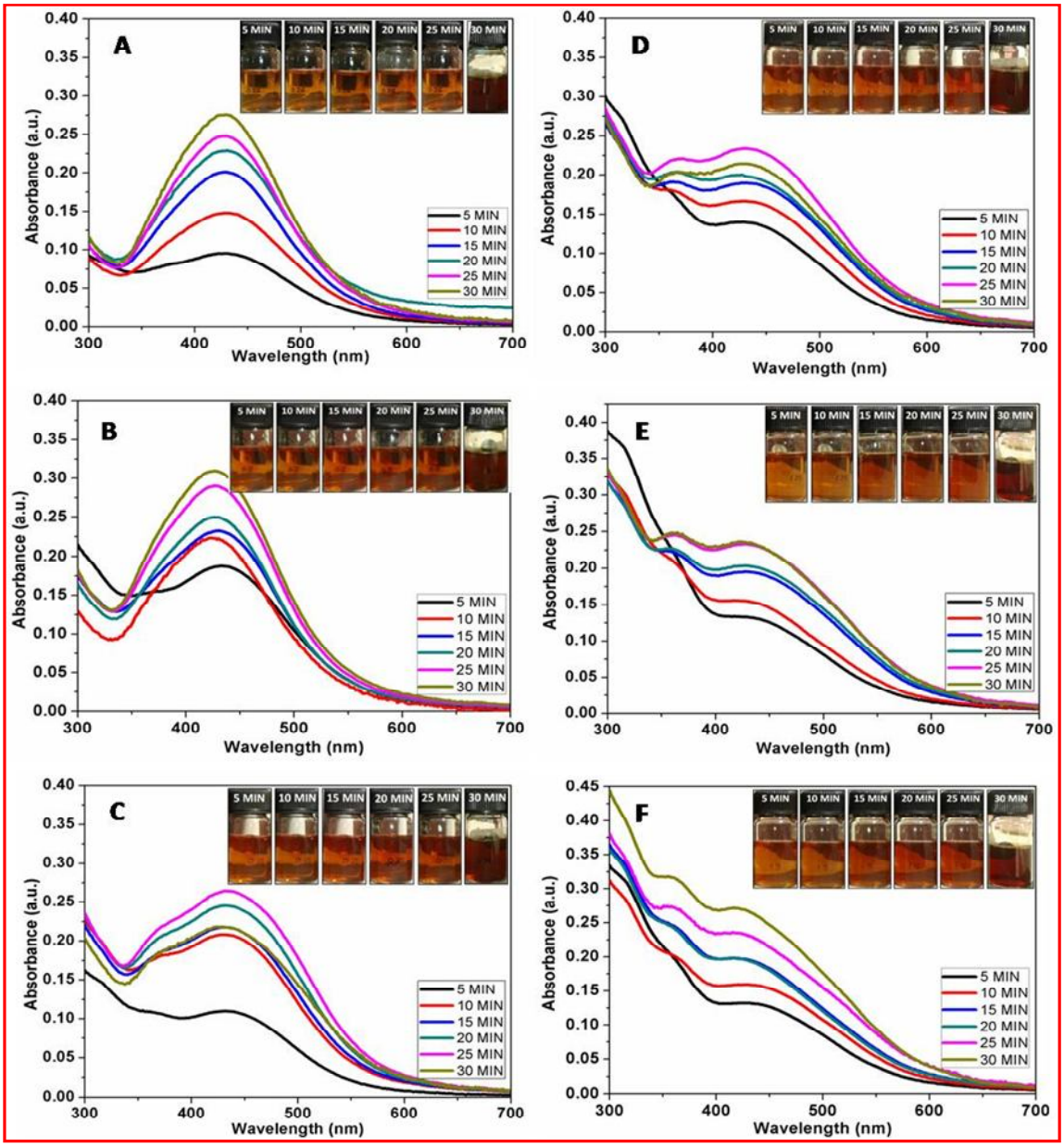

Figure 4.3 UV–visible absorption spectra of AgNPs recorded as a function of AEC inoculum dose from 2.5% to 15.0%; (A) 2.5%, (B) 5.0%, (C) 7.5%, (D) 10.0%, (E) 12.5%, and (F) 15.0% AEC and their respective increase in intensity and color change with the proceeding of time from 5 to 30 min (conditions; 1 mM $AgNO_3$ concentration and reaction time in bright sunlight exposure from 5 to 30 min)

It was observed that the reduction of Ag^{+} to Ag^{0} began to start within 10 second. Although, initially the intensity of the SPR band was not sharp, the observed SPR bands at 442 nm indicated the beginning of AgNPs synthesis. The screened samples at each 5 second showed 2-3 SPR band with polydispersed AgNPs up to 35 second. Thereafter, a single SPR band with roughly monodispersed AgNPs by 40 second of sunlight exposure continued to be single and sharp up to 30 min. Therefore, after 40 second of exposure, the samples were screened at each 5 min of interval. The gradual increase in intensity of the SPR band up to 30 min showed that the reduction of silver ion was in progress while further no change in SPR band intensity confirmed the completion of the reaction (Prakash *et al*. 2013) (**Fig. 4.4**).

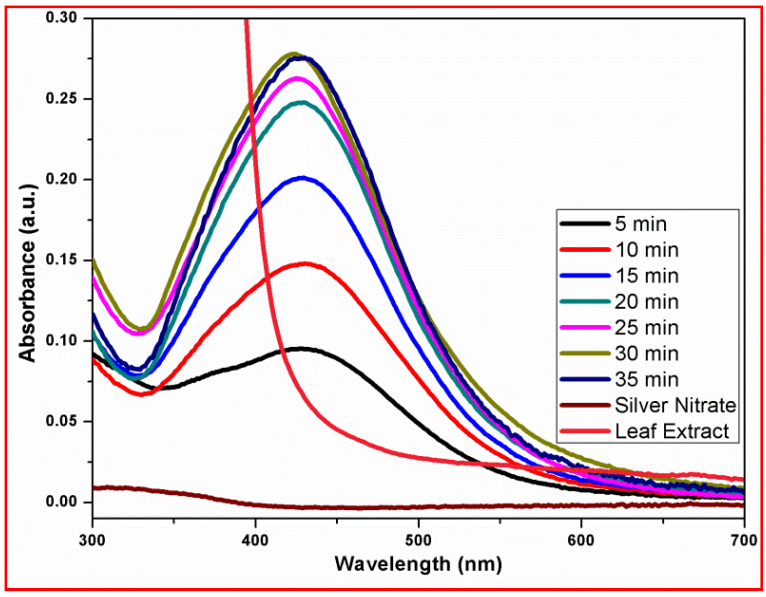

Figure 4.4 UV–visible absorption spectra of AgNPs recorded in bright sunlight at 5, 10, 15, 20, 25, 30 and 35 min (from 5 to 35 min) showing establishment of equilibrium

During continued increase in SPR band and reduction of AgNPs, the blue shift was also observed from 442 nm to 436 nm up to 40 second. This blue shift was also continued from 5 to 30 min for each inoculum doses. It was observed that after 30 min of exposure, the

SPR band of 2.5%, 5.0%, 7.5%, 10.0%, 12.5% and 15.0% blue shifted from 436 nm to 428 nm, 435 to 425 nm, 437 nm to 435 nm, 438 nm to 435 nm, 441 to 429 nm and 443 nm to 423 nm. This blue shift indicated that as the sunlight exposure time increased the size of the AgNPs decreased (Hou *et al*. 2013, Birla *et al*. 2013). Both the control solutions of $AgNO_3$ and AEC did not develop the characteristic reddish brown colors as well as any SPR band. This supports that the abiotic reduction of $AgNO_3$ did not occur under the used reaction conditions. On the basis of these results, 30 min of bright sunlight exposure time was considered as optimum for photoinduced biosynthesis of AgNPs. Thus, 30 min sunlight exposure time was fixed for further experiments.

4.3.2.2 AEC inoculums dose

The quantity of reductant in the reaction mixture was optimized by varying the AEC inoculum dose (v/v) from 2.5% to 15.0% while keeping other parameters constant at 30 min of sunlight exposure time and 1 mM $AgNO_3$ concentration in the reaction mixture. The results are shown in **Figure 4.3A-F**. It is clear from the figure that the intensity and sharpness of single SPR band of each time interval continued to increase up to 5.0% AEC inoculum dose. The increase in intensity indicated that the biosynthesis of AgNPs increased with increase in AEC inoculum dose up to 5.0% (Gade *et al*. 2014, Mandal *et al*. 2006). The appearance of single and sharp SPR band denoted that the synthesized AgNPs were spherical in shape which was also confirmed by FE-SEM and HR-TEM analysis. While using 7.5 % AEC, although the intensity of the SPR bands increased up to 30 min but it was lower and broader than 5.0% AEC. When the inoculum dose further increased from 10.0%, to 15.0% the intensity of single SPR bands gradually decreased, became broader and got split into two shoulder SPR bands at a lower wavelength. The decline in intensity and broader SPR band

indicated the decreased synthesis with bigger sized AgNPs due to agglomeration whereas the appearance of shoulder peak indicated the synthesis of anisotropic AgNPs (Jagtap and Bapat 2013). The intensity of the shoulder peaks of 10.0% to 15.0% AEC continued to increase to 30 min. This increase in the intensity of shoulder peak indicated that as the AEC inoculum dose increased the synthesis of anisotropic AgNPs also increased (Kumar *et al*. 2016b).

4.3.2.3 $AgNO_3$ concentration

The effect of $AgNO_3$ concentration on the synthesis of AgNPs was screened in the range of 1 mM to 6 mM at 5.0% AEC inoculum dose and 30 min of sunlight exposure time. **Fig. 4.5A-F** represented the SPR bands of AgNPs at different $AgNO_3$ concentrations i.e. 1 mM, 2 mM, 3 mM, 4 mM, 5 mM, and 6 mM after 30 min of sunlight exposure which was at 428 nm, 442 nm, 442 nm, 442 nm, 444 nm and 444 nm respectively. It was observed that the color of reaction mixture became darker with gradual increase in $AgNO_3$ concentration at each time interval for the fixed reaction time. Firstly, the intensity and sharpness of the SPR band of each $AgNO_3$ concentration increased up to 4 mM at each time interval and then ceased and become broader. The increase in SPR band intensity up to 4 mM indicated that as metal ion concentration increased, the synthesis of AgNPs also increased (Bar *et al*. 2009). The simultaneous shifting of SPR bands with advancement of time as well as metal ion concentration was also observed. The SPR band of 1 mM blue shifted from 437 nm to 428 nm with the advancement of time which indicated the decrease in AgNPs size (Bhui *et al*. 2009, Kathiresan *et al*. 2009).

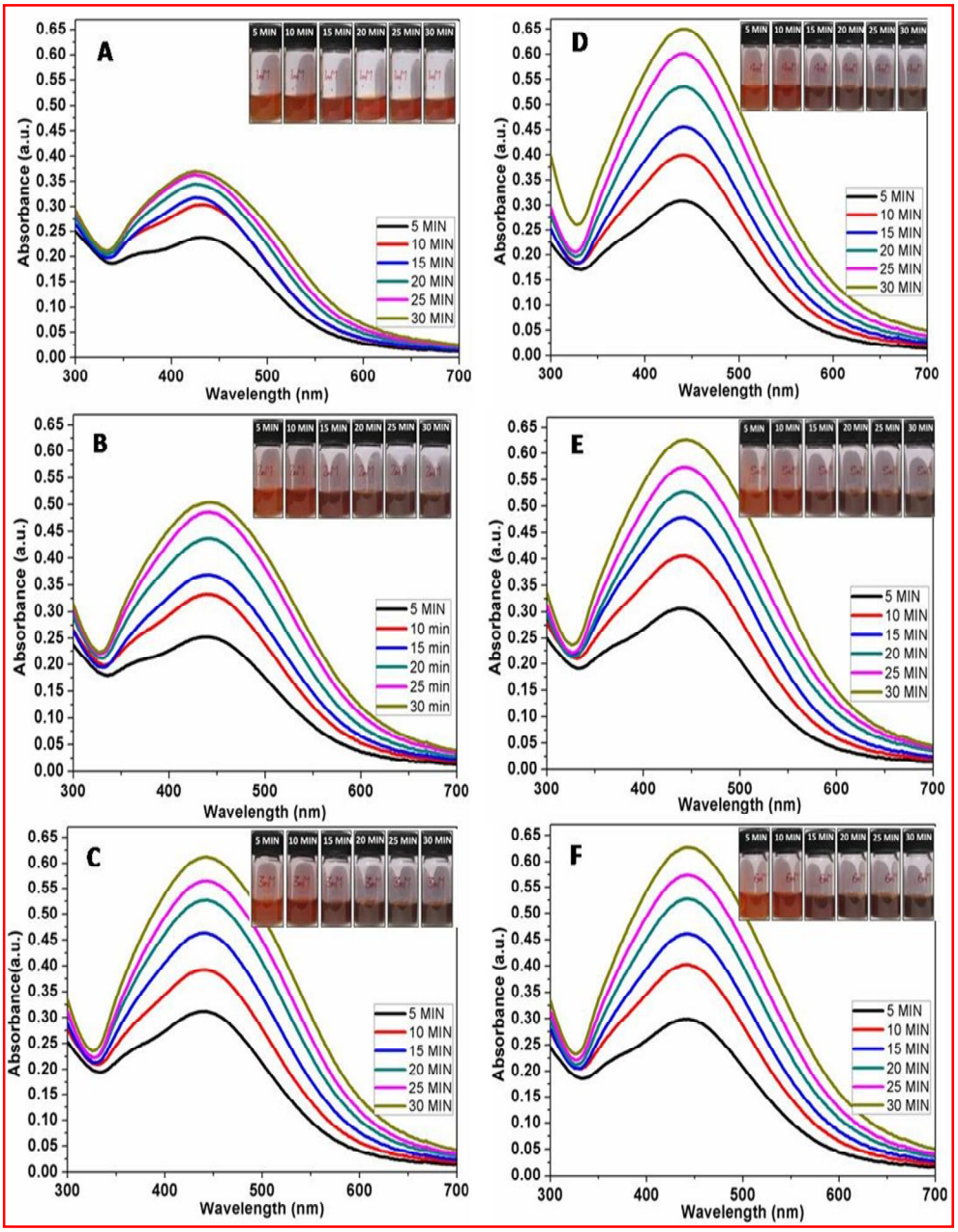

Figure 4.5 UV–visible absorption spectra of AgNPs recorded as a function of different $AgNO_3$ concentration varied from 1 mM to 6 mM (A) 1 mM, (B) 2 mM, (C) 3 mM, (D) 4 mM, (E) 5 mM, and (F) 6 mM and their respective increase in intensity and color change with the proceeding of time from 5 to 30 min (conditions; AEC inoculum dose 5.0% and sunlight exposure from 5 to 30 min)

Whereas the SPR band of 2 mM, 3 mM, 4 mM, 5 mM and 6 mM slightly red shifted from 440 nm to 442 nm, 440 nm to 442 nm, 441 nm to 444 nm, 440 nm to 443 nm and 440 nm to 442 nm respectively which indicated the increase in AgNPs size. The SPR band of 1 mM to 6 mM red shifted from 427 nm to 442 nm after fixed reaction time which also indicated the increase in particle size with increase in metal ion concentration (Bhui *et al*. 2009, Kathiresan *et al*. 2009, Vanaja *et al*. 2013). Thus, it is clear that $AgNO_3$ concentration governs the particle size distribution (Mock *et al*. 2002). Therefore, 4 mM $AgNO_3$ concentration was chosen as optimal for current study in order to get smaller sized particles with controlled growth for better antimicrobial and antioxidant activity.

4.3.3 Mechanism involving AgNPs biosynthesis

Many researchers have already reported the presence of tannin, polyphenols, resins, glycosides, steroids, flavonoids and many alkaloids through the phytochemical analysis of *C. bonplanadianum* leaf extract (Jeeshna *et al*. 2011). Tannins, flavonoids and sugars act as an effective reducing agent while proteins, glucose and some other phytochemicals present in leaf extract act as capping agent for AgNPs synthesis (Kumar *et al*. 2016b, Mathur 2014).

On the basis of the phytochemical profile of *C. bonplanadianum*, photo-inductive effect of sunlight on AgNPs biosynthesis and FTIR analysis of AEC, TA, pre-annealed AgNPs and post-annealed AgNPs, we have proposed a probable mechanism of AgNPs biosynthesis through AEC. Although, the presence of several phytochemicals in the AEC may provide many alternative reduction routes yet, the availability of tannins, a polyphenol to act as reductant was comparatively higher due to the prominent quantity of these chemicals in AEC (Kumar *et al*. 2016b, Prakash *et al*. 2013, Kathiresan *et al*. 2009). **Scheme 4.1** represented the molecular structure of tannin where one of its enol forms is shown by **'v'**.

We have proposed a stepwise mechanism of AgNPs synthesis. When the AEC was added into the $AgNO_3$ solution, the OH group of polyphenolic compound (tannin) present in AEC bound with Ag^+ and formed the Ag^+/AEC complex. Since, the results clearly showed that the biosynthesis of AgNPs was driven by the photocatalytic effect of sunlight.

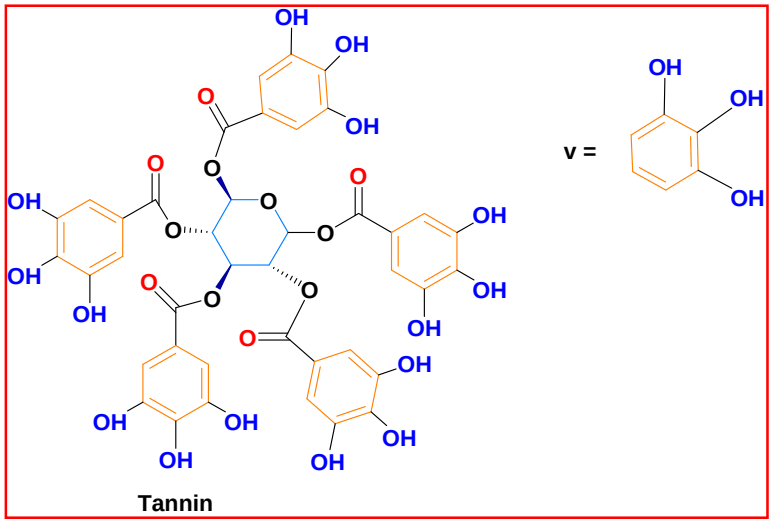

Scheme 4.1 Molecular structure of tannin

The first step involved the photoactivation of Ag^+/AEC complex where the OH group of AEC produced hydrated electrons by debonding of OH group after absorbing the photons of light, putting strong evidence after the sunlight induced synthesis of AgNPs. The second step involved the reduction of Ag^{1+} to Ag^0 by the hydrated electrons produced earlier. The concentration of silver atoms (Ag^0) continued to increase with the continued reduction of $AgNO_3$. When the increased concentration of Ag^0 atoms exceeded the critical supersaturation, the Ag^0 started to nucleate and formed the crystal nuclei (step III). The formation of these crystal nuclei led to the decrease in concentration of Ag^0 atoms below to

the critical supersaturation where the whole process is dominated by the growth of nuclei to form nanoclusters because of no longer increase in number of crystal nuclei (IV).

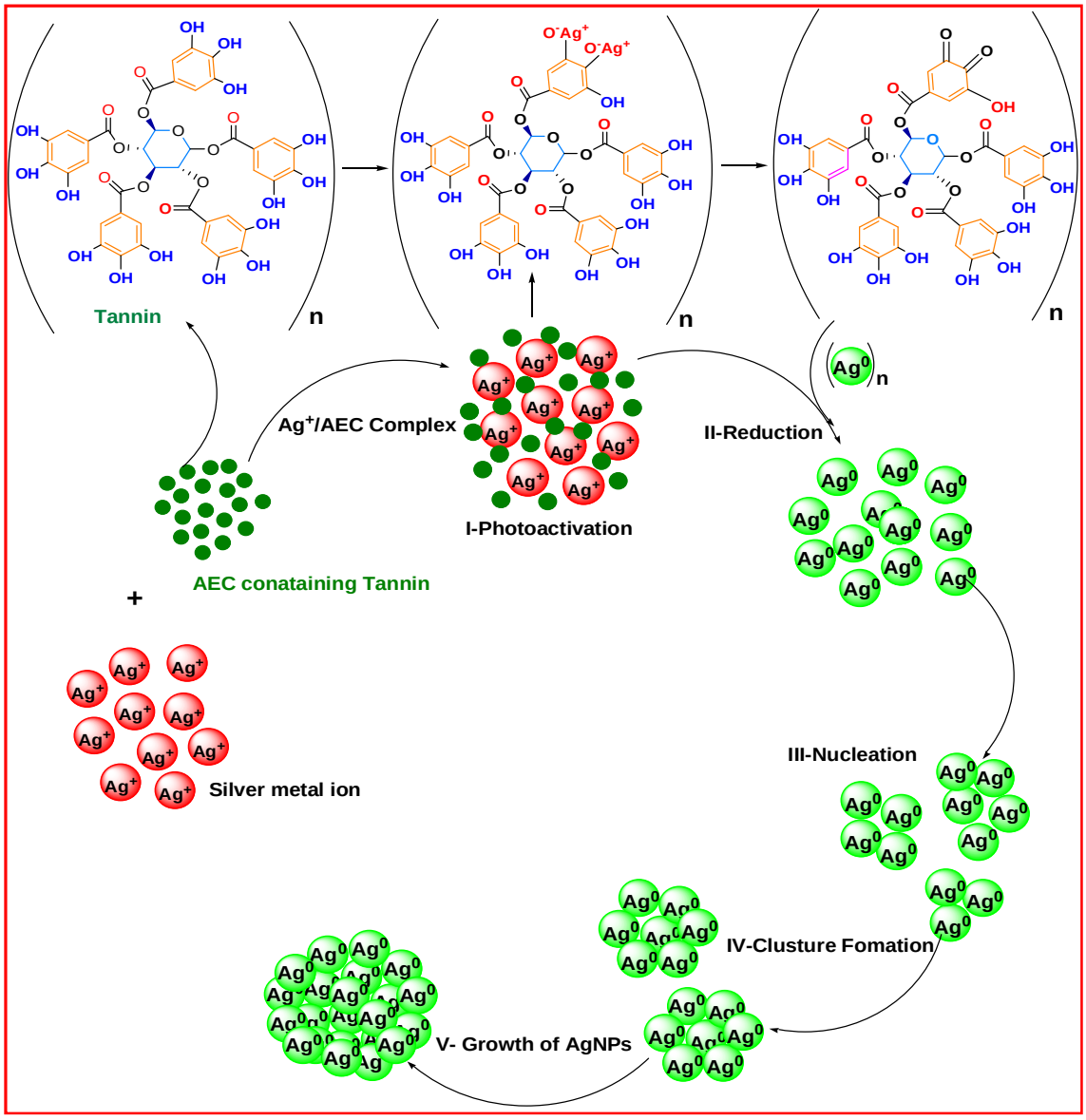

Scheme 4.2 Schematic representation of various steps of AgNPs synthesis where the enol form of 'n' number of polyphenolic groups of 'n' number of tannin present in AEC formed complex with Ag^+ and further reduced the n[Ag^+] to n[Ag^0] which simultaneously undergo nucleation, cluster formation and AgNPs growth. While reduction, the enol form change into quinonoid from by releasing 'n' number of electrons

The growth of the nanoclusters further decreased the concentration of Ag^0 atoms below the saturation level which stopped the growth of nanoclusters and finally aggregated to form AgNPs (V). The fourth step involved the simultaneous growth of nanopaticles by the aggregation of nanoclusters. This photocatalytic action of sunlight can further be strengthened by the fact that many flavin binding proteins, terpenols and other phytochemicals were also photoresponsive, they either itself can easily donate the electrons in the presence of sunlight or can induce other compounds to do the same (Gade *et al*. 2014). In this case proteins, sugars or some other phytochemicals act as stabilizers for AgNPs. This prediction can be evident from the IR analysis which clearly indicated the involvement of –OH and $–NH_2$ groups in synthesis and stabilization of AgNPs. **Scheme 4.2** showed the involvement of n(OH) of n(tannin) present in AEC to form n(Ag^0) atom and their nucleation which is followed by the nanoclusters formation and growth of AgNPs.

4.3.4 Characterization of AgNPs

After primary confirmation of biosynthesis through UV-visible spectrophotometer further the optimized AgNPs obtained at 30 min of sunlight exposure time, 4 mM $AgNO_3$ concentration and 5.0% of AEC inoculums dose was characterized through SEM, EDX, TEM, SAED, XRD, FTIR, AFM and XPS analysis.

Figure 4.6A showed the SEM images of the AgNPs. For the SEM analysis, one drop of synthesized colloidal AgNPs was casted over the thin sheet of the aluminium and dried under table lamp for two hrs. The SEM images showed the discrete distribution of mono dispersive spherical shaped AgNPs throughout the mass of samples. The elemental composition of AgNPs was confirmed through SEM equipped Energy Dispersive X-ray

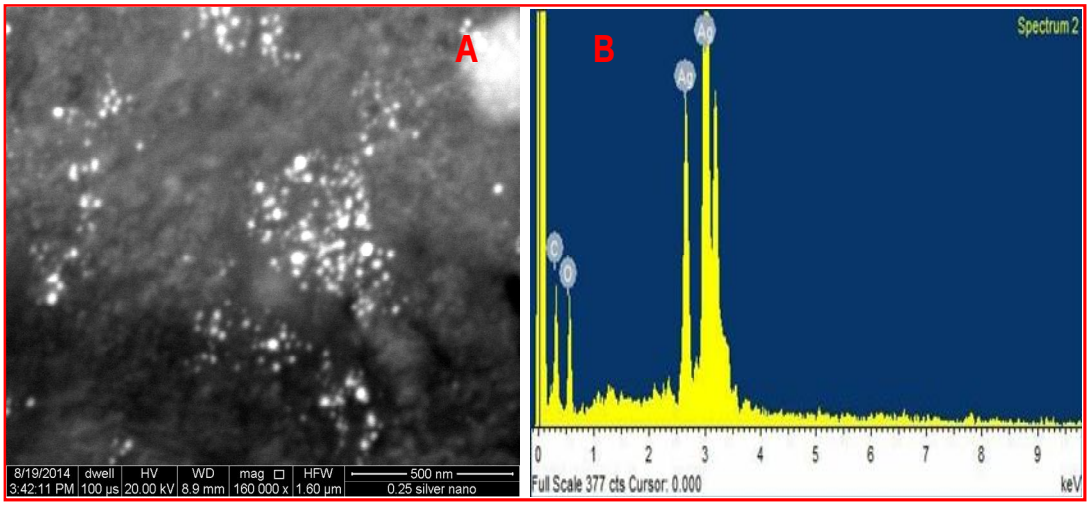

Figure 4.6 (A) SEM images of colloidal AgNPs synthesized by 5.0 % AEC, 4 mM $AgNO_3$ and 30 min of sunlight exposure time, (B) EDX spectrum of AgNPs

The energy dispersive spectra of EDX analysis showed a prominent spectral signal of silver (Ag) approximately at 3 keV, which corresponded to the absorption of metallic silver nanocrystallites due to SPR of AgNPs (**Figure 4.6B**). The presence of distinct spectral signals for carbon and oxygen were also recorded which corresponded to the biological materials like proteins, carbohydrates and other biomolecules of AEC present in the vicinity of AgNPs (Jayaseelan *et al*. 2013).

The TEM analysis explored the exact size and shape of biosynthesized AgNPs. The typical TEM images of biosynthesized AgNPs at different magnification are shown in (**Fig. 4.7A-B**). The TEM images revealed the abundance of roughly spherical shaped AgNPs with size ranging from 4 to 46 nm. A size distribution histogram of AgNPs corresponding to TEM image represented that maximum AgNPs were in the range of 15 nm to 25 nm having an average size distribution of 19.4 nm (**Fig. 4.7C**). The selected area electron diffraction

(SAED) pattern of AgNPs colloid is shown in **Figure 4.7D**. The typical SAED pattern with bright circular rings confirmed that the biosynthesized AgNPs were crystalline in nature.

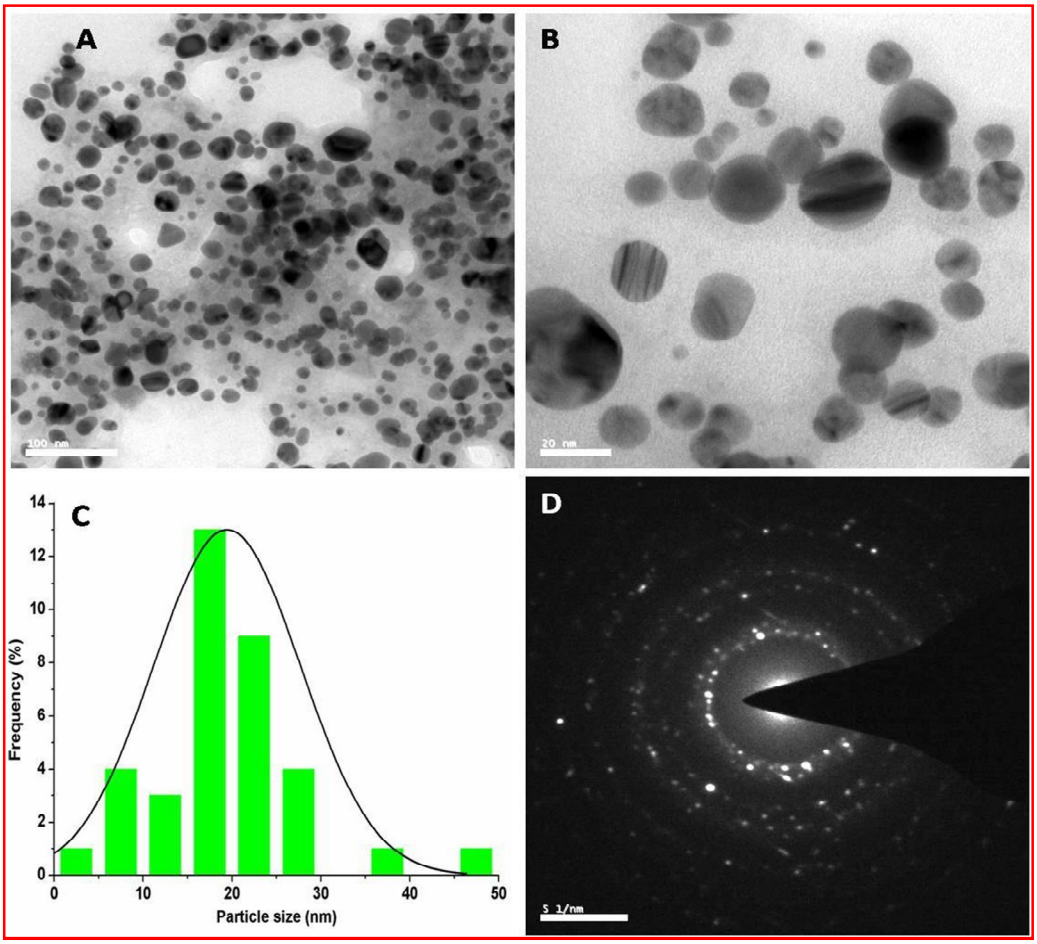

Figure 4.7 (A-B) TEM images of optimized AgNPs at different magnifications, (C) AgNPs histogram showing size distribution, (D) SAED patterns of crystalline AgNPs

The crystalline powder obtained from the optimized AgNPs was used for XRD analysis. The XRD pattern of the pre-annealed and post annealed AgNPs is shown in **Figure 4.8**. The XRD data were collected in the angular range $20° \leq 2\theta \leq 80°$, where the diffraction peaks of both the spectra observed at 2θ were 38.09°, 44.04°, 64.26° and 77.26°. These Peaks were well matched with standard diffraction data of AgNPs (JCPDS file no.040783) and

attributed to the (111), (200), (220) and (311) Bragg reflections which corresponded to the crystalline planes of the face-centered cubic (fcc) crystal lattice of metallic silver.

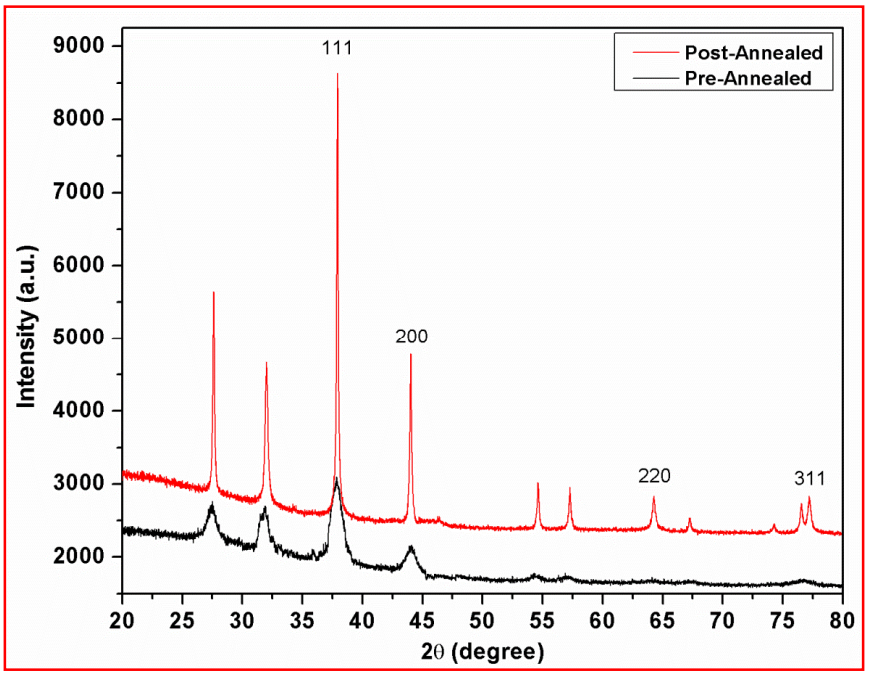

Figure 4.8 X-ray diffraction patterns of pre-annealed and post-annealed AgNPs

The average estimated crystallite size of the AgNPs was in the range of 22.7 nm. These results were consistent with the size of nanoparticles obtained from the HR-TEM analysis as illustrated above. It was noticed that the XRD peaks of pre-annealed AgNPs was broader and less intense which was due to smaller crystallite size. The increase in peak width results into decrease in size of the crystallites and intensity. The peaks of post-annealed AgNPs were taller and much narrower than pre-annealed because of periodicity of larger crystallite domain which reinforced the diffraction of X-ray (Moon *et al*. 2005).

The FTIR analysis was performed to explore the identity of the biomolecules involved in the synthesis and stabilization of AgNPs. The FTIR spectra of TA, AEC, pre-annealed AgNPs and post-annealed AgNPs are represented in **Fig. 4.9** where the FTIR spectra of AEC was compared with the FTIR spectra of TA to confirm the presence of characteristics groups of tannin in AEC. The FTIR spectrum of AEC was also taken as a control to compare the reduction in intensity and shifting of characteristic peaks in FTIR spectra of synthesized pre-annealed AgNPs. The FTIR spectrum of post-annealed AgNPs was used to corroborate the capping of AgNPs with the moieties present in the AEC.

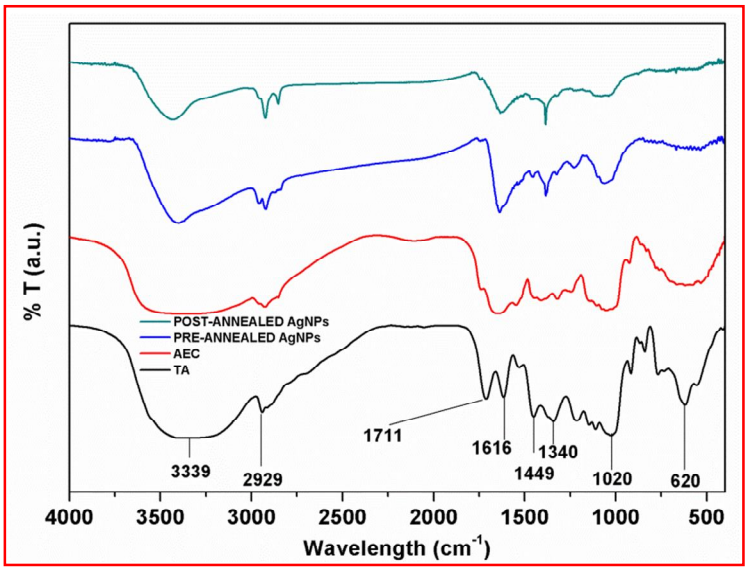

Figure 4.9 Typical FTIR spectra of tannic acid, AEC, pre-annealed and post-annealed AgNPs

The FTIR spectra of pure TA showed the characteristics band at 3339 cm^{-1} (υ_s of OH), 2939 cm^{-1} (υ_s of C=C-H), 1711 cm^{-1} (υ_s of CO), 1616 cm^{-1} (υ_s of C=C), 1449 cm^{-1} (υ_s of C=C), 1340 cm^{-1} (υ_s of C=C) 1020 cm^{-1} (υ_s of O-C) and 620 cm^{-1} (υ_b = bending vibration) which were almost similar to that of AEC which confirmed the presence of tannin like

moieties (polyphenolic) in the AEC. The FTIR spectra of pre-annealed AgNPs showed characteristic bands similar to those of AEC except some shifting which indicated that the biomolecules present in AEC played an important role in synthesizing and stabilizing AgNPs. Both the spectra showed a shifting in following peaks: from 3483 to 3405 cm^{-1} (band due to υ_s of OH of the glucose, phenolic compounds and υ_s of NH of the proteins), 2925 to 2918 cm^{-1} (υ_s of C=C-H), 1653 to 1638 cm^{-1} (due to amide I band υ_s of C=O, amide II band υ_s of NH), 1413 to 1384 cm^{-1} (due to benzene υ_s of C=C), 1035 to 1064 cm^{-1} (υ_s of O-C) (Bai and Abraham 2002, Huang *et al*. 2010, Nakano *et al*. 2001, Oo *et al*. 2009). These findings indicated the involvement of hydroxyl, carboxyl, amino and amide groups of phytochemicals of AEC in the AgNPs biosynthesis. These groups can majorly be contributed by tannins, glucose and protein fraction of AEC. The post-annealed FTIR spectra of AgNPs exhibited the reduction in the intensity of the characteristics peak which indicated the loss of organic moieties adhered to the surface of the AgNPs while stabilization.

The atomic topological structure of biosynthesized AgNPs was studied through AFM technique. The 2D and 3D topographical view and roughness profile of AgNPs are represented in **Fig. 4.10A, B & C** respectively. For the AFM analysis, a single drop of colloidal AgNPs was casted over cover slip and dried under table lamp for two hrs. The **Figure 4.10C** represented that the maximum profile peak height and maximum valley depth were 18.79 nm and 13.11 nm respectively whereas the average roughness of the height profile was 4.84 nm.

The XPS analysis was used to characterize the elemental composition of the synthesized AgNPs. The survey scan spectrum of AgNPs is shown in **Figure 4.11A.**

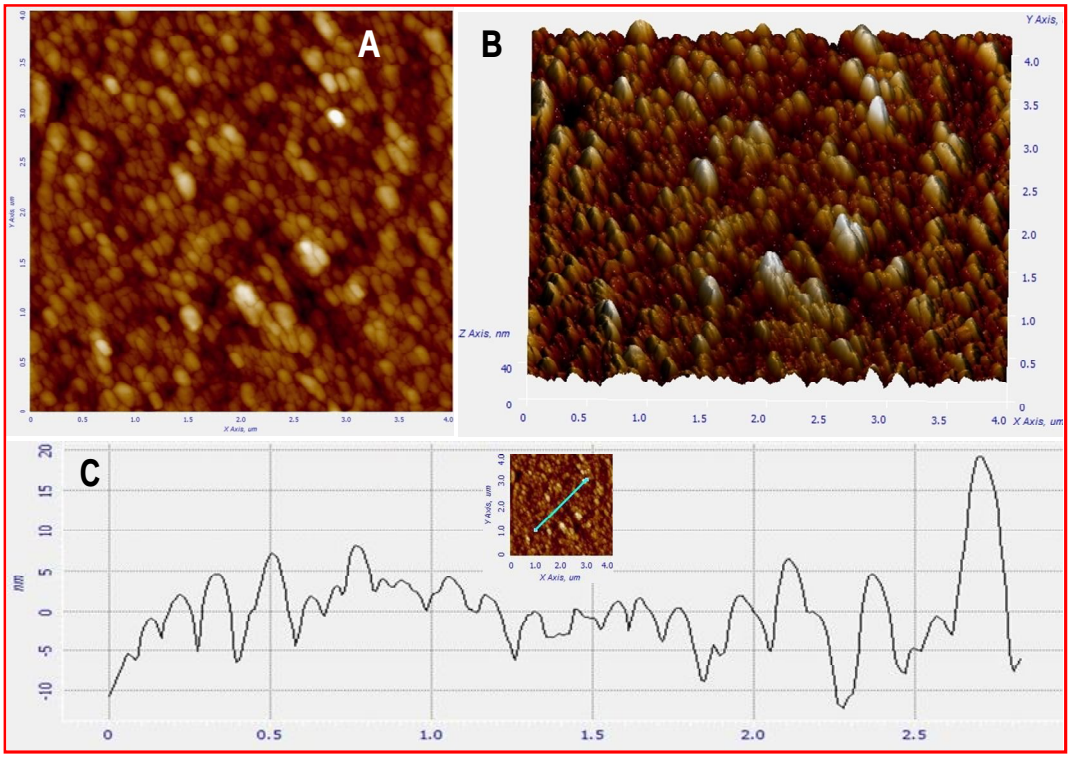

Figure 4.10 AFM images of biosynthesized AgNPs showing (A) lateral, (B) 3D view, and (C) roughness profile

The survey spectrum exhibited the peaks corresponding to C 1s, Ag 3d and O 1s which depicted C, Ag, and O as a major element present in the sample. The peaks of C and O clearly indicated the presence of biological moieties involved in the synthesis process. The core level C 1s spectrum (**Figure 4.11B)** have two Gaussian peaks at 286.4 and 288.0 eV assigned to COC/COH and C=O/C–Ag respectively (Sang *et al*. 2016). **Figure 4.11C** showed the Ag 3d core level spectrum of AgNPs. The Ag 3d spectrum of Ag corroborated two peaks at 375.70 and 369.70 eV which corresponded to the binding energies of Ag $3d_{3/2}$ and Ag $3d_{5/2}$ respectively. The splitting of the 3d doublet of Ag is 6.02 eV, indicating the formation of metallic AgNPs (Ag^0) (Liang *et al*. 2014). The O 1s core level spectrum fitted

into an individual component is represented in Figure **4.11D** which showed only one peak of the O 1s signal at 532. 6 eV which was due to the C=O groups.

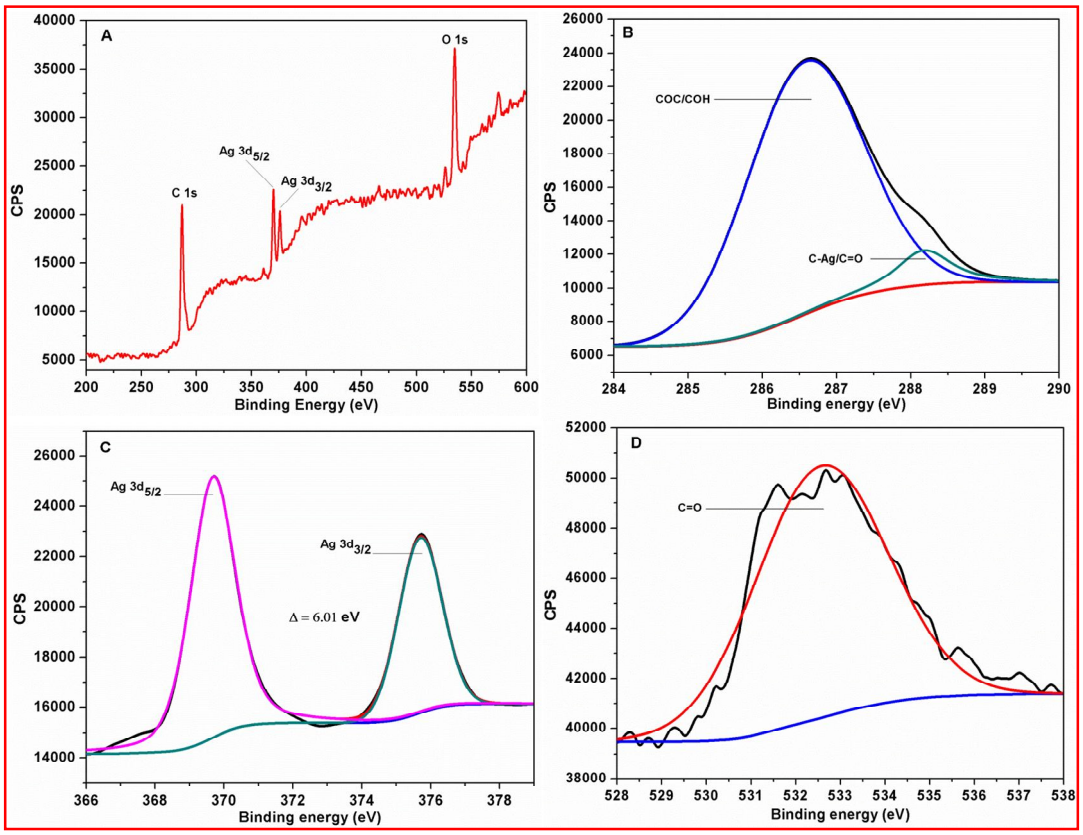

Figure 4.11 XPS spectra of AgNPs (A) wide scan spectra, (B) C 1s spectrum, (C) Ag 3d spectrum, and (D) O 1s spectrum

4.3.5 Stability of AgNPs

The stability of AgNPs obtained at optimum condition i.e. 30 min sunlight exposure time, 5.0 % inoculum dose and 4.0 mM $AgNO_3$ concentration was monitored up to 9 months. The samples were kept at room temperature and pH of the AgNPs colloid was 7.2. **Figure 4.12** represented the SPR band profiles at different time intervals. The broadening and

decrease in intensity of SPR band, visual precipitation, as well as pH were taken into account for the stability monitoring.

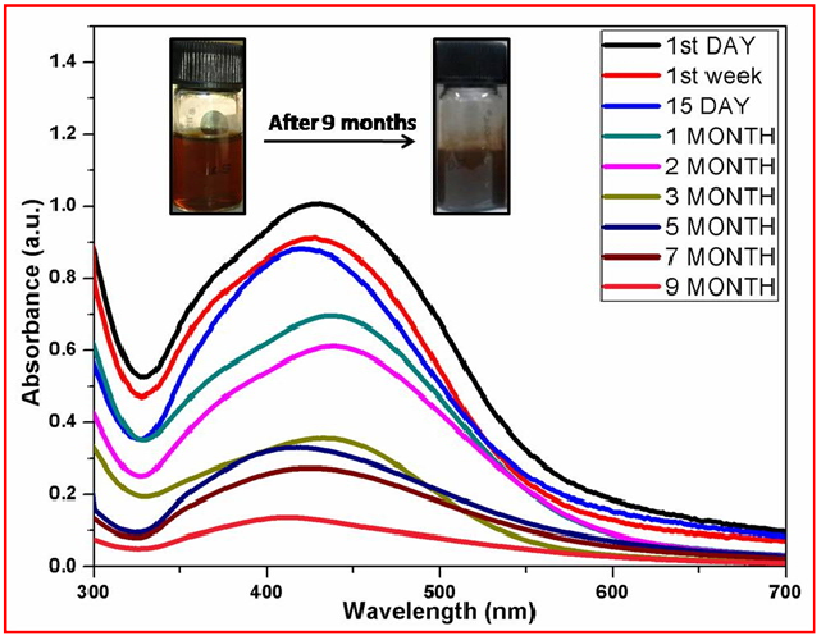

Figure 4.12 UV–visible absorption spectra of optimized AgNPs showing the monitoring of stability up to 9 months of incubation period at neutral pH and room temperature, (Inset Figure 4.12) change in color from transparent brown to turbid and dark brown

It was noticed that the intensity of the SPR band decreased and became broader. The decreasing and broadening of the SPR band indicated that colloidal AgNPs get aggregated, become bigger sized and settled as the time advanced. It was found that during 9 months of period the pH of the reaction mixture was decreased from 7.2 to 5.1. Based on the pH effect it can be concluded that at lower pH, over nucleation has occurred due to which the AgNPs get agglomerated and settled down and hence became unstable (Vanaja *et al*. 2013). The samples having AEC inoculum doses more than 5.0% get precipitated at the bottom within

the first week. These characteristics showed that the stability of AgNPs decreased with increase in inoculums dose and incubation of time period.

4.4 Colorimetric detection of iron (Fe^{3+})

The colorimetric sensing property of AEC synthesized AgNPs was investigated separately for different metal ion including, Fe^{3+}, Fe^{2+}, Pb^{2+}, Cd^{2+}, Co^{2+}, Zn^{2+}, Ni^{2+}, Al^{3+}, As^{3+}, Cu^{2+}, Hg^{2+}, and Mn^{2+} at the same concentration of 200 µL. **Figure 4.13A** shows the UV-visible absorption spectra of AgNPs after introduction of various metal ion. The color of the **Inset Figure 4.13A** and UV-visible absorption spectra clearly showing that the most of the metal ion did not cause significant change in color as well as UV-visible absorption spectra. However, when Fe^{3+} and Hg^{2+} were added, a significant decrease in absorption intensity was observed, efficiently with Fe^{3+}. On the basis of this results it can be concluded that AEC synthesized AgNPs can be used as selective sensing material of Fe^{3+}. **Figure 4.13B** showed the change in absorbance after adding different metal ion solution in to the AgNPs solution.

For the investigation of Fe^{3+} sensitivity, different concentration of Fe^{3+} was added into the AgNPs solution. **Figure 4.13C** shows the decrease in intensity of the SPR band as well as color of the AgNPs solution. It was observed that the intensity of the SPR band and color of the AgNPs decreased gradually while increasing the concentration of Fe^{3+} in the AgNPs solution. The linear relationship between the SPR band intensity and Fe^{3+} concentration within the range of 0-225 µL is shown in inset **Figure 4.13D**. The fitting line can be expressed as: $\Delta A=0.0008\ [Fe^{3+}] - 0.015$ (ΔA A_0-A, where A_0 and A represented the intensity of the SPR band in the absence and presence of Fe^{3+} respectively, $[Fe^{3+}]$ refers to the concentration of Fe^{3+} having linear regression coefficient (R^2) of 0.997.

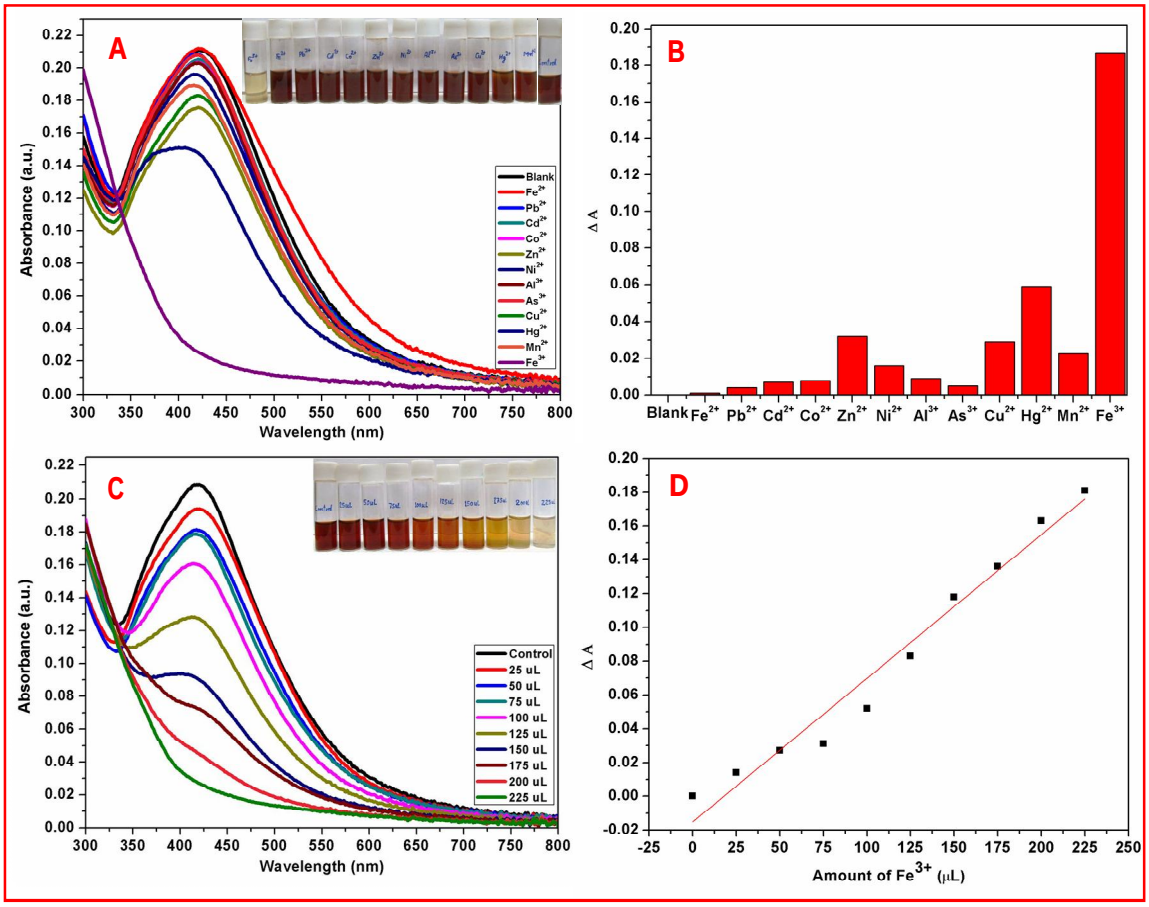

Figure 4.13 (A) Change in UV-visible absorption spectra of AgNPs with addition of 200 µL (1×10^{-3} M) solution of different metal ions (including Fe^{3+}, Fe^{2+}, Pb^{2+}, Cd^{2+}, Co^{2+}, Zn^{2+}, Ni^{2+}, Al^{3+}, As^{3+}, Cu^{2+}, Hg^{2+}, Mn^{2+}), (B) selectivity of AgNPs towards Fe^{3+}, (C) UV-visible absorption spectra of AgNPs with addition different volume of Fe^{3+} ranged from 25 µL to 225 µL, (D) linear relationship between the change in UV-visible absorption and Fe^{3+} concentration

In addition to this, the change in color of the AgNPs solution can be helpful in the qualitative determination of Fe^{3+} as depicted in **Inset Figure 4.13A** and **4.13C**. When the different metal ion were added in AgNPs solution, the colorlessness of only Fe^{3+} indicated the high selectivity of AEC synthesized AgNPs towards Fe^{3+} detection. The color of AgNPs

solution is also sensitive to the amount of added Fe^{3+} as shown in **Inset Figure 4.13C**. Therefore, AEC synthesized AgNPs can be used for the naked eye detection of Fe^{3+}.

4.4.1 Mechanism of detection of Fe^{3+}

Generally, the colorimetric detection of transition metal ions is achieved by using fluorescent nanoparticles due to their strong interaction which resulted into quenching effect (Guo and Irudayaraj 2011). Non-fluorescent AgNPs have also showed the colorimetric sensing potential towards Hg^{2+} based on their alloy formation and anti-aggregation mechanism (Duan *et al*. 2014). In the present investigation the mechanism of the colorimetric detection of Fe^{3+} is proposed on the basis of colorlessness of AgNPs solution, decrease in SPR band intensity and TEM image obtained after addition of Fe^{3+} into AgNPs solution. It was observed that when Fe^{3+} was added in to the AgNPs solution, it became colorless and the SPR band intensity diminished without red-blue shift. The colorlessness of the AgNPs solution and diminishing SPR band suggested the reduction in amount of AgNPs in the solution without change in the size. The presence or absence of the AgNPs in the solution after the addition of Fe^{3+} was further confirmed by TEM image and UV-visible spectrum of the centrifuged bottom solution (**Fig. 4.14**). It is clearly obvious from the **Figure 4.14** that neither the UV-visible spectra nor TEM image showed the presence of AgNPs in Fe^{3+} added solution. On the basis of these results, we have proposed an oxidation-reduction mechanism of colorimetric detection of AgNPs as shown in **Scheme 4.3**. As per this mechanism, when Fe^{3+} is added in to the AgNPs solution, the Ag^0 get oxidized into the Ag^+ which lead to the decomposition of AgNPs and resulted in to the colorlessness of the AgNPs solution, decrease in SPR band intensity and decrease in the amount of AgNPs in the solution as well.

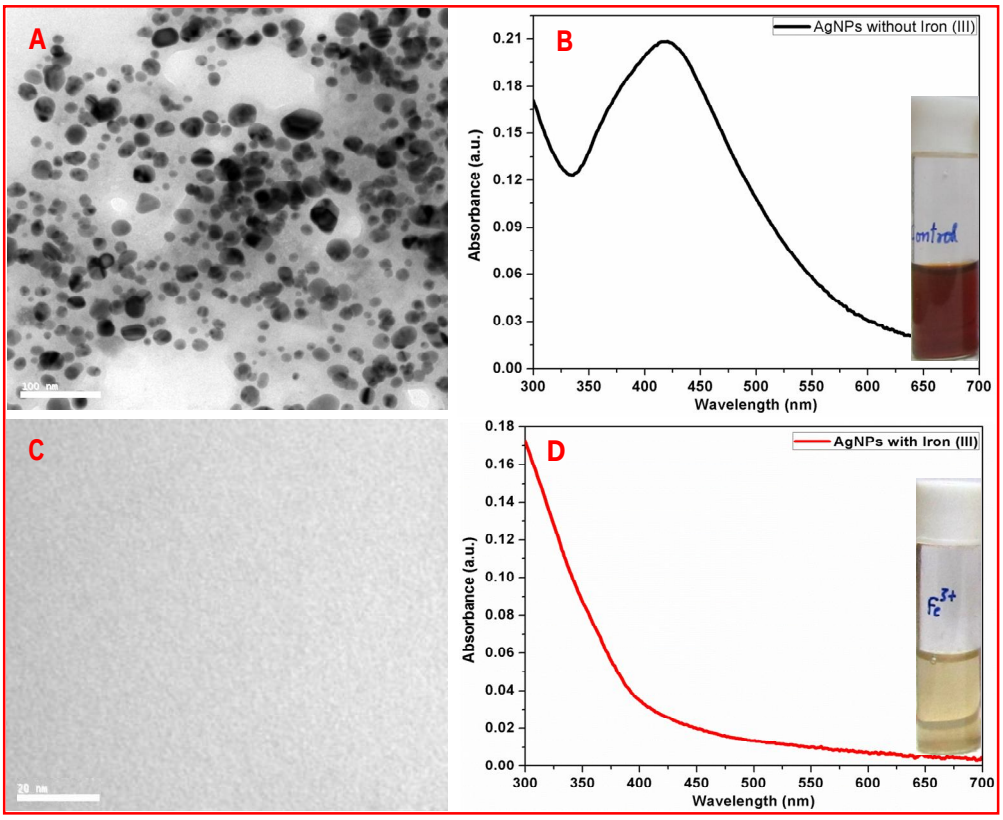

Figure 4.14 TEM images of AgNPs and corresponding UV-visible spectra without and with Fe^{3+}

The possibility of the oxidation-reduction reaction between AgNPs and the Fe^{3+} is also showed by previous studies (Gao *et al.* 2015).

4.5 Antimicrobial activity of AgNPs

The biosynthesized AgNPs showed excellent antimicrobial activity against *E. coli* and *S. aureus* which showed maximum inhibition at 0.53 µg/mL and 0.64 µg/mL respectively, for all bacterial strains tested, indicating their stronger antimicrobial activity. The antimicrobial activity by using AgNPs, aqueous $AgNO_3$, AEC against *E. coli* and *S. aureus* were shown in **Inset Figure 4.15B** and **Table 4.1**.

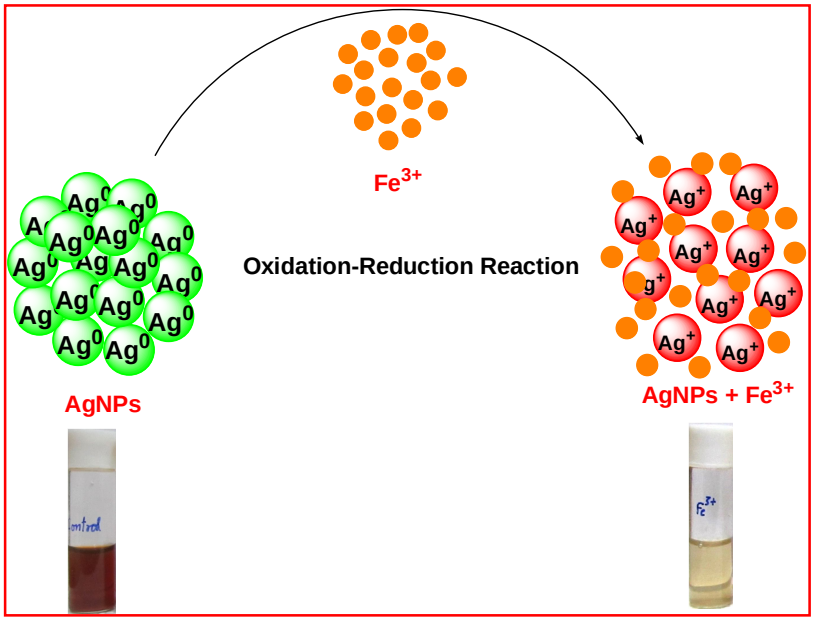

Scheme 4.3 Oxidation-reduction reaction involved in colorimetric detection of Fe^{3+}

The cell wall of Gram-positive bacteria contains a thick peptidoglycan layer consisting of linear polysaccharide chains cross-linked by short peptides resulting into a rigid structure leading to difficult penetration of the AgNPs compared to the Gram-negative bacteria where the cell wall possesses thinner peptidoglycan layer (Shrivastava *et al*. 2007). It could be presumed that high bactericidal activity was due to the silver (Ag^0) released from nanoparticles that act as reservoirs for the Ag^+ bactericidal agent. Such changes in the membrane structure of bacteria as a result of the interaction with silver cations lead to the increased membrane permeability of the bacteria (Dibrov *et al*. 2002, Sondi and Salopek-Sondi 2004). Yu-sen *et al*. explained that in general, silver ions from AgNPs are believed to become attached to the negatively charged cell wall of the bacteria and rupture it which leads to denaturation of protein and finally cell death (Yu-sen *et al*. 1998). The attachment of either silver ions or nanoparticles to the cell wall caused the accumulation of envelope protein

precursors which resulted in dissipation of the proton motive force. On the other hand, Lok *et al*. elucidated that AgNPs exhibited destabilization of the outer membrane, rupturing of the plasma membrane and thereby causing depletion of intracellular ATP (Lok *et al*. 2008). As per Sarkar *et al*. report, the AgNPs demonstrated greater bactericidal efficiency on *E. coli* and *S. aureus* as compared to penicillin (Sarkar *et al*. 2007). It is known that silver has a greater affinity to react with sulfur or phosphorus containing biomolecules in the cell. Thus, sulfur-containing of the membrane or inside the cells and phosphorus containing elements like DNA are the most preferential sites for AgNPs binding (Bragg and Rainnie 1974, Russell 1999).

4.5.1 Cell viability

Time-dependent antibacterial behavior was examined in the presence of AgNPs and higher activities were determined in our early tests. The cells of *E. coli* and *S. aureus* were incubated for 4 hrs after adding a concentration of AgNPs as 0.53 µg/mL AgNPs for *E. coli* and 0.64 µg/mL for *S. aureus*. The loss of cell viability of *E. coli* and *S. aureus* was counted at hourly intervals. The loss of cell viability of *E. coli* increased steadily with extension of incubation time as shown in **Figure 4.15A**. *E. coli* cells encapsulated with 0.53 µg/mL AgNPs showed loss of cell viability up to 0.8 after zero hr, 19.3 after 1 hr, and increased to 51.4, 72.8 and 93.5 after 2, 3, and 4 hrs, respectively. The cells of *S. aureus* encapsulated with 0.64 µg/mL showed viability up to 0.9 after zero hr, 20.1 after 1 hr, 47.4 after 2 hrs which further increased to 63.3 after 3 hrs and 86.8 after 4 hrs, respectively. Both cells showed a higher rate of death after incubation for 1-2 hr and complete death during last 3-4 hrs after encapsulation with AgNPs. There was no loss of cell viability in the control sample of *E. coli* and *S. aureus* in both conditions.

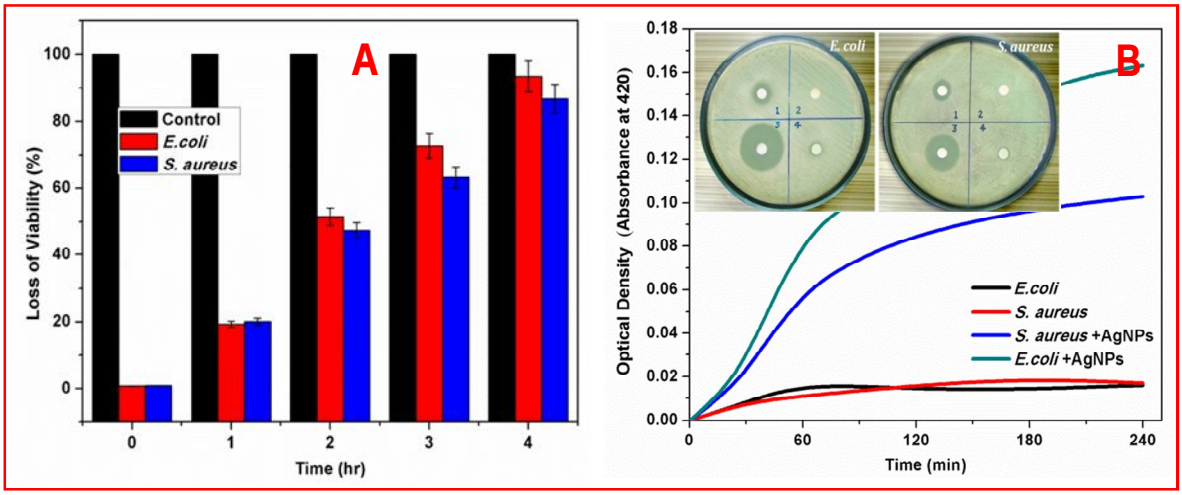

Figure 4.15 (A) *E. coli* and *S. aureus* (10^6 colony forming units/mL) cells were treated with AgNPs at 37 °C for 4 hrs at 200 rpm. Cell-viability test were performed by the colony-counting method and expressed as a percentage of control, (B) optical density (OD) curves indicating the absorption of ONP, (Inset Figure 4.15B) disc diffusion method showing inhibition zone produced by using (1) AEC, (2) Buffer solution, (3) AgNPs, and (4) aqueous $AgNO_3$ (each 20 µL against *E. coli* and *S. aureus*)

Table 4.1 Antimicrobial activity of AgNPs, aqueous $AgNO_3$ and AEC

Microorganism	Control	$AgNO_3$	AEC	AgNPs (5 µg/mL)
Escherichia coli	0	0.8	13	30
Staphyloccocus aureus	0	0.5	15	23

4.5.2 Antimicrobial mechanism of AgNPs

The β-D-galactose glycoside bond present in sugar, fat and lactose get hydrolyzed by a special enzyme β-D-galactosidase (Kornfeld and Kornfeld 1985). The β-D-galactosidase, especially from *E. coli* has substrate specificity for the hydrolysis of ONPG (Qin *et al*. 2014). The penetration of AgNPs at the cell wall disrupted the membrane integrity and subsequently mediated the release of functional enzymes such as β-D-galactosidase from the bacterial cell

and finally killed the cell. The β-D-galactosidase present in the cytoplasm of *E. coli* cells gets leaked out after lysis of cells and then catalyzed the hydrolysis of ONPG in the solution. The product (ONP) of ONPG hydrolysis reaction has a characteristic absorption at 420 nm and hence spectroscopy method can be used to determine cell disruption of *E. coli*. The changes of absorption with time were measured as shown in **Fig. 4.15B** and at the same time two control samples were also measured at the same time intervals. From **Fig. 4.15B** it can be observed that the absorption of the blank system was nearly zero and it did not vary with time. The fact displayed that the membrane of *E. coli* cell was intact and no β-D-galactosidase is released in controlled condition. The increased absorption at 420 nm with time clearly indicated that AgNPs has significantly disrupted the cell membrane of *E. coli* and caused to release the intracellular component, β-D-galactosidase. The OD curves were observed to have a higher level of cell disruption action which resulted into release of a high amount of β-D-galactosidase and its derived catalysis of ONPG to ONP. The experimental facts clearly indicated that AgNPs disrupted the cell membrane due to which the intracellular β-D-galactosidase is released. The absorption of ONPG hydrolysis reaction at 420 nm was increased up to 3 hrs which indicated that inhibition was continued up to 3 hrs while further no change in absorption indicated that the total inhibition was completed.

4.5.3 Cell morphology observation

The results obtained showed that the membranes of *S. aureus* and *E. coli* cells were intact before treatment with the AgNPs. **Figure 4.16A and C** showed the SEM images of untreated log phase *S. aureus* and *E. coli* cells which were typically round and rod shaped with smooth and intact cell walls respectively.

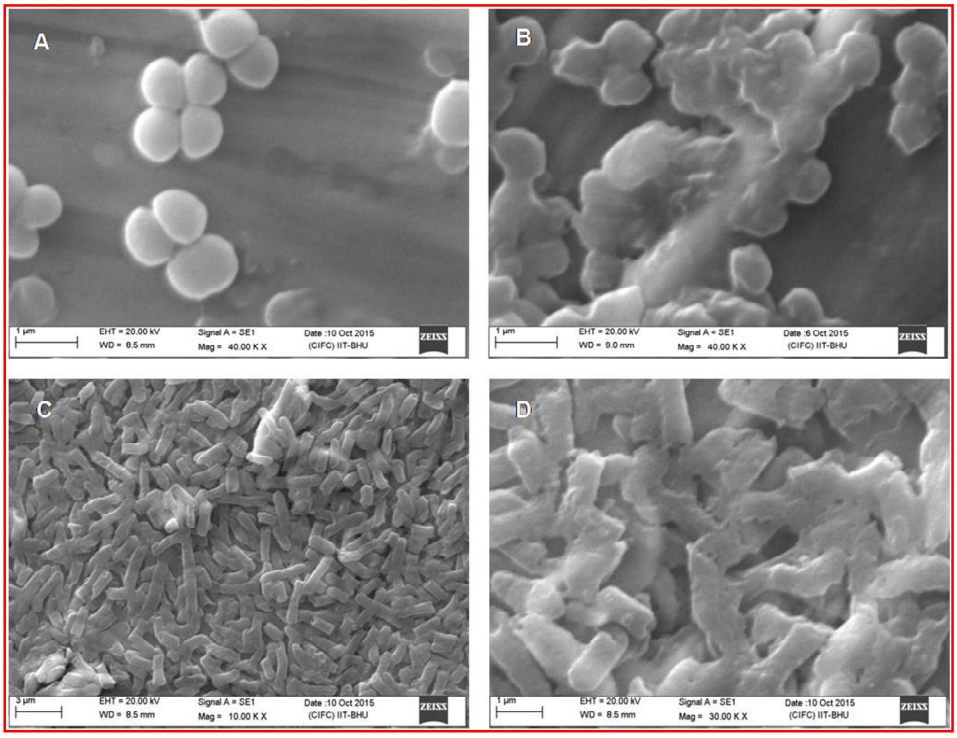

Figure 4.16 SEM images of (A and C) *S. aureus* and *E. coli* cells respectively without treatment, and (B and D) treated with AgNPs for 4 hrs

For investigating the effect on the number, shape and size, 1.68 µg/mL and 2.55 µg/mL AgNPs was added to the cells of *E. coli* and *S. aureus* and incubated for 4 hrs. After that, the cells of *E. coli* and *S. aureus* were collected and fixed systematically. It was found that the numbers of *E. coli* and *S. aureus* cells greatly decreased, cell walls became damaged and shape and size markedly changed for most *S. aureus* and *E. coli* cells **(Figure 4.16B and D)**. The strong adhesion between AgNPs and bacteria led to cell deformation and the loss of the original structure of the bacterium. The antibacterial properties of AgNPs severely destroyed the cell membrane.

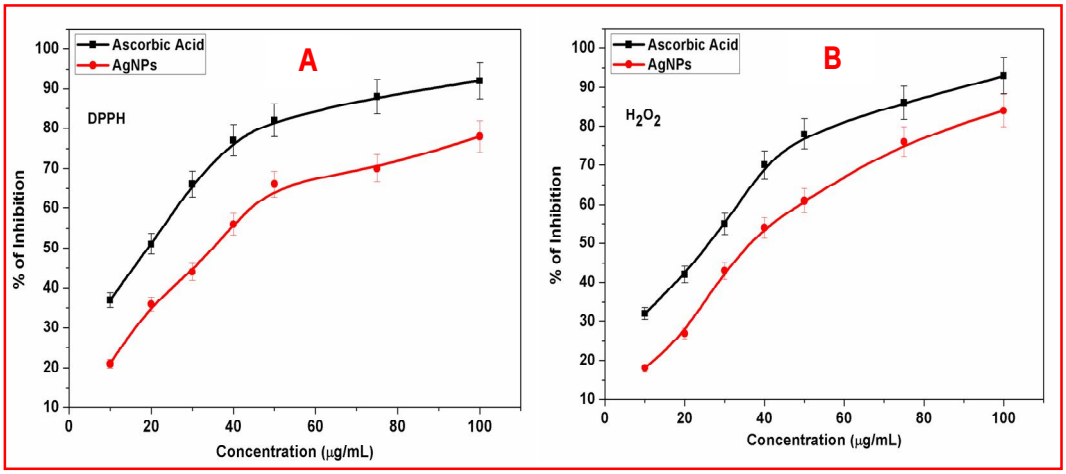

Figure 4.17 Antioxidant activity of biosynthesized AgNPs

4.6 Antioxidant activity

4.6.1 DPPH assay

DPPH, a more stable and standard free radical with a characteristic absorption at 517–520 nm was used to study the free radical scavenging activity of biosynthesized AgNPs. This free radical scavenging is based on the reduction of DPPH by accepting hydrogen or electron from donors. The DPPH reducing ability of the AgNPs was assessed primarily by observing color change where the decrease in absorption was taken as a measure of the extent of free radical scavenging. The DPPH scavenging assay exhibited effective inhibition activity of AgNPs when compared with the standard Ascorbic acid (**Fig. 4.17A**). The DPPH activity of the AgNPs was increased in a dose-dependent manner. However, the AgNPs exhibited more inhibition with 80 % scavenging activity of DPPH. As we have discussed earlier, while synthesis the AgNPs get protected by the stabilizing agents like proteins and other polyphenolic constituents present in the AEC. The AgNPs thus synthesized become a rich source of hydrogen. When the AgNPs was added to the stable free radical (DPPH) solution,

the color changed from violet to yellow. The change in color was observed due to the conversion of free radical (diphenypicrylhydrazyl) to non-free radical (diphenylpicryhydrazine).

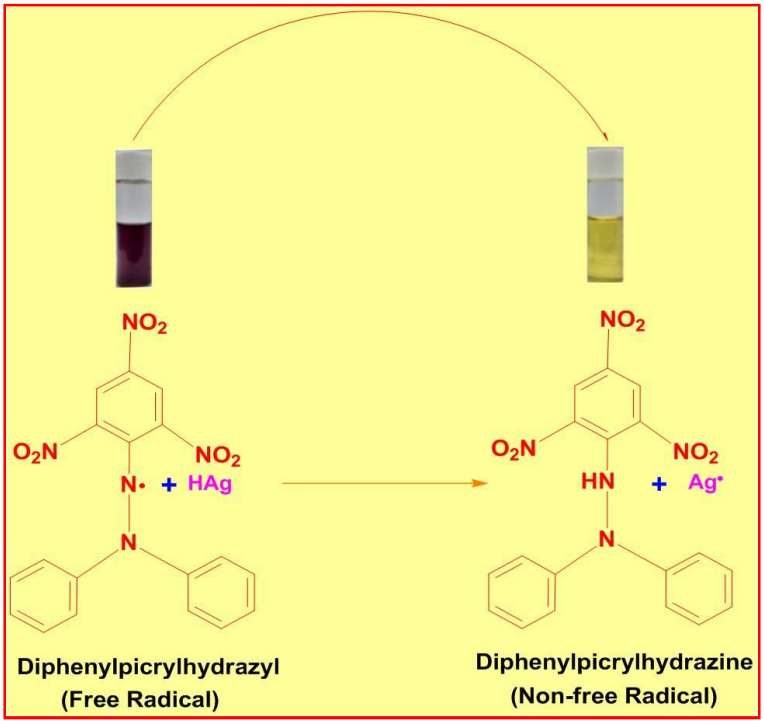

Scheme 4.4 Reduction of diphenylpicrylhydrazyl (stable free radical) into diphenylpicrylhydrazine (non free radical) via accepting the hydrogen atom

4.6.2 Measurement of H_2O_2 scavenging assay

In living systems, the accumulation of H_2O_2 leads to the development of oxygen free radicals like peroxide and hydroxyl radicals which cause enormous damage to cell membranes. The H_2O_2 scavenging activity of AgNPs was quantified spectrophotometrically using ascorbic acid as a standard which is shown in **Figure 4.17B**. At the concentrations of 100 µg/mL, 90 and 80 % inhibition were found respectively for the AgNPs and ascorbic acid.

Moreover, the H_2O_2 free radical scavenging was higher than those obtained for DPPH. Interestingly, the AgNPs exhibited comparatively better scavenging activity than ascorbic acid. In the presence of H_2O_2, the dispersed AgNPs can induce reactive oxygen species like hydroxyl radicals. H_2O_2 inside a cell at a low dose can accelerate the dissolution of AgNPs and produce much stronger oxidative stress (He *et al*. 2012). AgNPs can produce greater accounts of H_2O_2 and induce enormous inflammasome formation because they can cause stronger seepage of cathepsins from the damaged lysosomes and efflux of K^+ ions may contribute to the production of superoxide and H_2O_2 in the membranes of mitochondria (Pick and Mizel 1981). Our results were in good accordance with an earlier report on the H_2O_2 scavenging effect of AgNPs synthesized by AEC.

4.7 Conclusion

In the present study a very simple, one step photoinduced green route have been developed for the optimum synthesis of highly stable and spherical shaped AgNPs for the selective colorimetric detection of Fe^{3+}. The developed photoinduced route was found to be very rapid and efficient to initiate AgNPs synthesis within seconds without any instrumental support or external energy supply like heating and stirring which remained stable for more than 9 months. The process was optimized through one factor at a time approach and the optimum conditions were found to be 4 mM $AgNO_3$ concentration, 5.0% (v/v) of AEC inoculum dose and 30 min of sun light exposure time. Most of the AgNPs were spherical and ranged between 4 nm to 46 nm having an average size distribution of 19.4 nm. Polyphenols and proteins were concluded as possible reductant and stabilizing agents respectively. During the evaluation of antimicrobial activity, AgNPs showed greater potential against gram-negative bacteria. The results revealed that the biosynthesized AgNPs were free radical

scavengers and acted as primary antioxidants also. A probable mechanism for current biosynthesis of AgNPs, Fe^{3+} detection, antibacterial and antioxidant activity was also proposed on the basis of facts and results. Overall, the developed photoinduced route is an excellent, eco-friendly and economically viable approach for the rapid synthesis of optimized stable AgNPs in a suitable size range for the selective Fe^{3+} detection, antimicrobial and antioxidant application.